In Situ Patterning of Microfluidic Networks in 3D Cell-Laden Hydrogels

*Nathalie Brandenberg and Matthias P. Lutolf**

Cells in the body reside in complex, tissue-specific three-dimensional (3D) microenvironments, termed extracellular matrices (ECM), that control their behavior and orchestrate their interaction with other tissue components to facilitate tissue development, function, and repair.[1] These microenvironments are highly dynamic since cell behavior often needs to rapidly respond to the changing physiological needs of the tissue and organism. A key mechanism to robustly control cellular dynamics is the tightly regulated presentation of cell signaling molecules in space and time. For example, during the development or regeneration of an organ, specific signaling molecules termed morphogens are secreted by cells from a restricted region of the tissue ('source') from where they diffuse to form concentration gradients.[2] Cells respond differentially to concentrations of these signals, resulting in distinct patterns of development and behavior.

Microfluidic technology offers unprecedented means to control exceptionally small amounts of fluids, making it ideally suited to build in vitro systems emulating the spatiotemporally complex signaling dynamics found in nature.[3] However, microfluidic technology has been largely limited to two-dimensional (2D) cell-culture applications and is inadequate for long-term cell culture in biologically relevant extracellular environments.[4] Moreover, most microfluidic systems are either fabricated from relatively nonbiological materials such as poly(dimethylsiloxane) (PDMS) or they are static, i.e., their architecture is predefined and thus not adaptable to dynamic biological signaling within a native tissue.

Efforts have been made to engineer microfluidic networks directly within cell friendly 3D hydrogels, but existing platforms are based on laborious processes that require several post-processing steps and offer little flexibility in design.[5–8] Alternatively, advanced biomaterials approaches are being explored to generate spatiotemporally complex signaling microenvironments for 3D cell culture. To this end, synthetic polymer hydrogels have been interfaced with innovative photochemistry to precisely modulate their characteristics in space and time through the controlled application of a light beam (e.g., ref. [9]). However, this approach limits itself to biomolecule patterns that are static, unlike those in native tissues.

We surmised that laser photoablation could be exploited to fabricate, if desired during cell culture, functional 3D microfluidic networks within hydrogels. Indeed, nano- or femtosecond pulsed lasers provide enough energy (≈80–150 mW and 500–900 mW, respectively) to break down covalent bonds and have been used for micromachining of hard materials such as glass and silicon.[10] Furthermore, previous studies reported the laser-based generation of cavities in nonpermissive hydrogels to promote 3D cell growth and migration.[11,12] Taking advantage of the ablative properties of focalized pulsed lasers, we report a new paradigm for creating functional 3D microfluidic networks at any time and location during a cell or tissue culture experiment. The concept is shown in **Figure 1**a,b: By scanning the area of a specified pattern, a custom-made network of channels can be fabricated and connected to a perfusion system, such as to generate functional microfluidic systems without any post-processing steps. In addition, the networks can be modified on demand during the culture in order to respond to needs of an evolving biological system (Figure 1b). As we demonstrate below, constructing microfluidic networks by direct laser writing offers a wide range of material possibilities, geometrical freedom, and the ability to introduce or modify existing microfluidic networks during the course of an experiment to manipulate cell behavior in situ in an unprecedented manner. We believe that this approach opens up many exciting avenues for tissue engineering, organs-on-chips, and organoid biology/technology.

To build functional microfluidic networks in hydrogels, we first designed simple custom-made PDMS mounts that can harbor a gel sample and interface the sample with inlets and outlets that enable perfusion (Figure 1c). The upper part of the hydrogel is covered with media, exhibiting an open cell-culture configuration akin to standard 3D culture in multiwell plates. The hydrogel is cast in the center chamber, and media, as well as factors of interest, can be flowed through the fabricated microfluidic networks by hydrostatic pressure differences,[7] on-chip peristaltic-valve-based systems, or conventional syringe pump-based systems.

To demonstrate the feasibility of our approach, we used the nanosecond-pulsed laser of a micro-dissection microscope (PALM MicroBeam system) to create various simple, planar patterns such as undulating (Figure S1a, Supporting Information) or ladder-shaped microfluidic channels in covalently crosslinked poly(ethylene glycol) (PEG) hydrogels (Figure 1d,e). An evaluation of channel stability by microscopy showed that geometries remain unchanged for at least 48 h, both with and without flow (≈1 µL min^{-1}; Figure S1b,c, Supporting Information). Importantly, microfluidic networks can be designed in

N. Brandenberg, Prof. M. P. Lutolf
Laboratory of Stem Cell Bioengineering
Institute of Bioengineering
School of Life Sciences
Ecole Polytechnique Fédérale de Lausanne (EPFL)
CH-1015 Lausanne, Switzerland
E-mail: matthias.lutolf@epfl.ch
Prof. M. P. Lutolf
Institute of Chemical Sciences and Engineering
School of Basic Sciences
Ecole Polytechnique Fédérale de Lausanne (EPFL)
CH-1015 Lausanne, Switzerland

DOI: 10.1002/adma.201601099

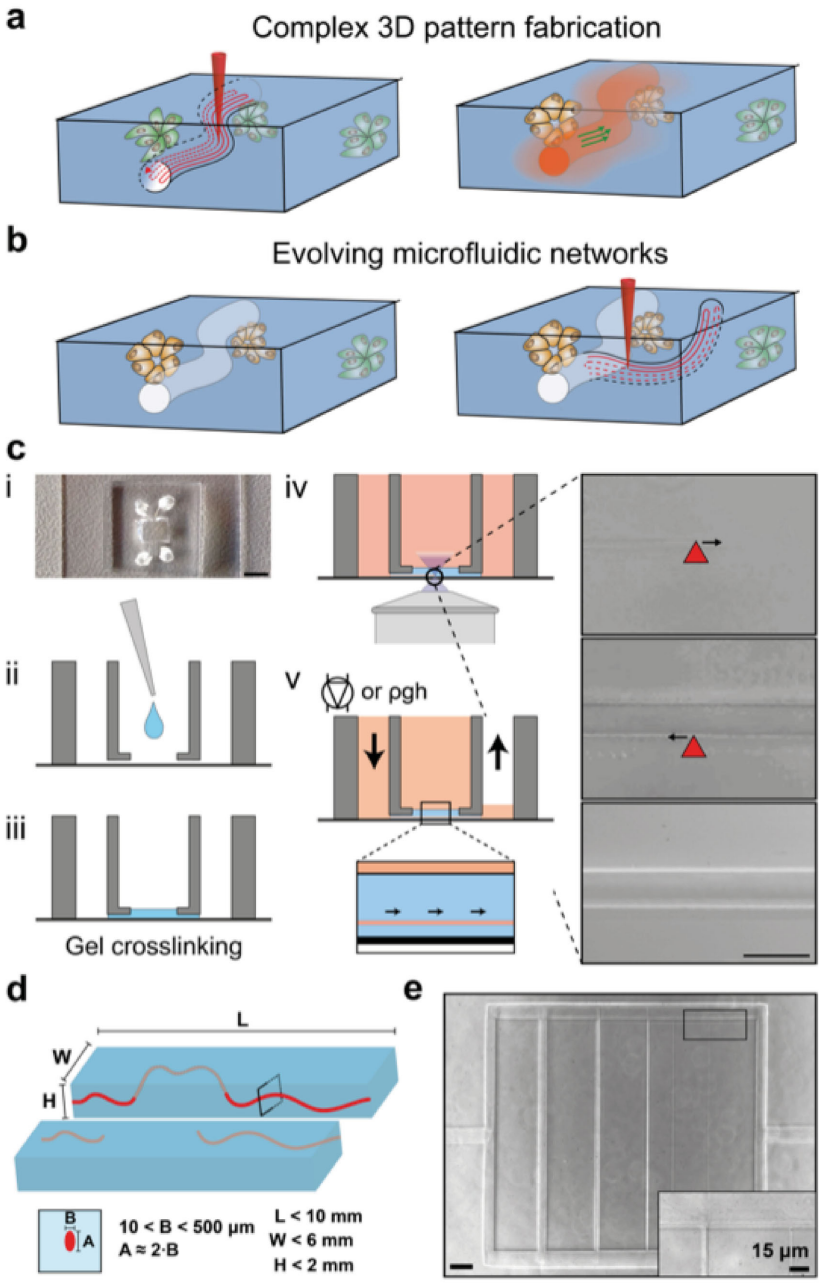

Figure 1. Schematic depiction of fabrication and use of in situ biomicrofluidics. a) Using the ablative properties of focalized nano- or femto-pulsed lasers, microfluidic channels are fabricated within cell-containing hydrogels by scanning the area of desired patterns. The microchannels are directly functional after the fabrication process. b) Additional microfluidic networks can be added on demand at any location and time during cell culture. c) Schematic overview of the fabrication process. (i) Representative image of the PDMS mount. Scale bar: 2 mm. (ii) The hydrogel precursor solution is pipetted into the PDMS mounts and (iii) incubated at 37 °C, 5% CO_2 for 20 min for crosslinking. The gel is then immersed with the appropriate medium and (iv) microfluidic networks are fabricated by scanning the area of a desired pattern with the laser. (v) Flow can be induced using hydrostatic-pressure-based or active-flow-based pumping systems. d) Schematic representation of the gel size range that can be processed as well as the resulting microfluidic network geometry. e) Any shape and curvature can be achieved with this method, such as ladder-like. Scale bars: 100 µm, unless specified.

numerous hydrogel types, including those made from natural ECM-derived proteins (gelatin, collagen type I, or fibrin) or polysaccharides (agarose, alginate), as well as various formulations of semisynthetic or fully synthetic hydrogels. The latter can span a wide range of mechanical properties, including ≈300 Pa in shear modulus (Figure S1d–f, Supporting Information), a particularly interesting range for 3D cell culture. To the best of our knowledge, such soft hydrogels cannot be micropatterned with previously reported methods, such as those based on micromolding.[7,8]

We then attempted to construct more complex microfluidic networks as a basis for fabricating sophisticated in vitro tissue models or permitting systematic studies of 3D cellular microenvironments. With the high resolution and reproducibility of controlling the coordinates of the automated microscope stage and the Z-position of a custom-made focus controller, we successfully fabricated perfusable microfluidic networks emulating blood flow through a flat capillary bed (**Figure 2**). Starting from a capillary-bed photograph, we generated a mask (Figure 2a) and path file (Figure 2b) that the laser could read to generate the corresponding microchannel structure (Figure 2c). When connected to a pumping system, we could demonstrate for the first time that very complex networks in hydrogels can be fully perfused (Figure 2d).

Furthermore, we could also form intricate 3D structures such as ramps, spirals, and other irregular shapes (**Figure 3**a,b and Movie S1 and S2, Supporting Information). Notably, the fidelity in 3D microfluidic patterning allowed us to superimpose different microfluidic networks without any tedious manual handling steps (Figure 3c). Flow experiments demonstrate the functionality of these microfluidic networks by efficiently transporting fluorescent molecules and polystyrene beads from the inlet to the outlet of the networks (Figure 3d and Movie S3, Supporting Information). Perhaps most interestingly, this strategy offers the possibility to readily modify microfluidic networks in situ, that is, during the time course of an experiment (Figure 3e,f). To the best of our knowledge, this aspect makes our approach unique among all hydrogel microfluidic strategies.

A thorough characterization of the mass transport phenomena in our hydrogel microfluidic networks is essential for developing useful in vitro cell culture and tissue models.

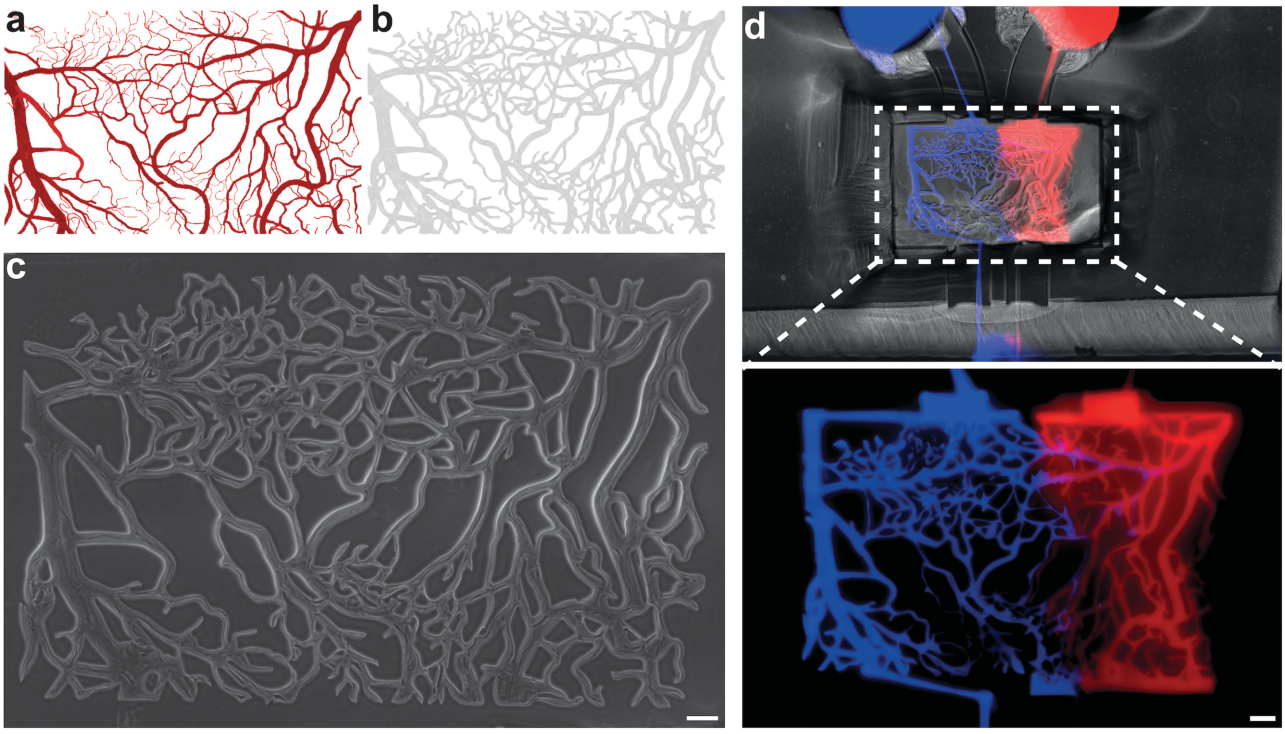

Figure 2. Complexity of the fabricated networks. a) Thresholded binary image of a capillary-bed photograph. b) Path file derived from the mask that the laser follows to fabricate the network. c) Resulting capillary-bed-mimicking microfluidic network prior to perfusion. d) These networks can be connected and perfused with different fluorescent molecules (e.g., alexa-647-labeled PEG and 2000 kDa fluorescein isothiocyanate (FITC)–dextrane), mimicking arteriovenous circulation. Scale bars: 100 μm.

As a tractable model system, we first analyzed the diffusion of fluorescent dextran (molecular weight ≈ 70 kDa) from a single source through covalently crosslinked PEG hydrogels (Figure S2, Supporting Information). Using curve fitting of the forming gradients (Figure S2a,c, Supporting Information), we estimated an effective diffusion coefficient (D_{eff}) for dextran of 1.8×10^{-7} cm^2 s^{-1}, which was then used to calculate the theoretical diffusion behavior based on convection–diffusion equations. Indeed, employing a finite element approach, the theoretical diffusion patterns corresponded very well with experimental data (Figure S2c,d, Supporting Information). This provided the basis for employing more complex perfusion patterns such as those based on a nonlinear delivery of factors such as a pulsed delivery (Figure S3, Supporting Information).

Given the importance of biomolecule gradients in controlling tissue development, we then aimed to construct a more physiological gradient system based on a source–sink mechanism (Figure S2e, Supporting Information). Indeed, by laser-etching and perfusing two parallel microfluidic channels in close proximity, one to deliver a biomolecule and the other to deplete it, we built highly stable source–sink gradient systems (Figure S2f,g, Supporting Information). Again, a strong correlation between theoretical and experimental diffusion properties was found in this delivery paradigm (Figure S2g,h, Supporting Information).

Finally, using a reactive fluorescent model compound (Alexa-546), we explored the possibility of establishing gradients of biomolecules which are tethered to the hydrogel matrix (Figure S2i, Supporting Information), a mode of biomolecule presentation that is physiologically relevant because ECM-binding in vivo can be beneficial for biomolecule activity.[13] By perfusing reactive maleimide–Alexa-546 for 2 h, we show that tethered gradients are established within synthetic PEG-based hydrogels bearing free thiol groups, and that these gradients remain stable over at least one week (Figure S2j–l, Supporting Information). Taken together, these experiments show that laser-based photoablation can be exploited to generate microfluidic networks with highly predictable mass transport behavior.

To demonstrate the relevance of our approach in biomedical research, we next sought to develop two in vitro models of biologically relevant processes (**Figure 4**a), namely, the induction of 3D chemotaxis and the establishment of an artificial blood-vessel network. To do so, we first assessed the compatibility of live cell culture with laser photoablation (Figure 4b). Importantly, the viability of 3D-encapsulated cells in bioactive PEG hydrogels one hour after channel fabrication was not significantly different than the cell viability in standard 3D culture in multiwell plates, or in the PDMS mounts in which microfluidic networks were not fabricated. Even a one to two cell diameters away (≈20 μm) from the laser-etched channels, we did not observe dying cells (Figure 4c).

Mesenchymal stem cells (MSCs) play key roles in tissue dynamics due to their ability to differentiate into cells of the mesodermal lineage, such as adipocytes, osteocytes, and chondrocytes, and also through modulation of the immune system.[14] However, MSC biology is still poorly understood, in part because physiologically relevant in vitro models to capture tissue-level MSC functionality are often inadequate.

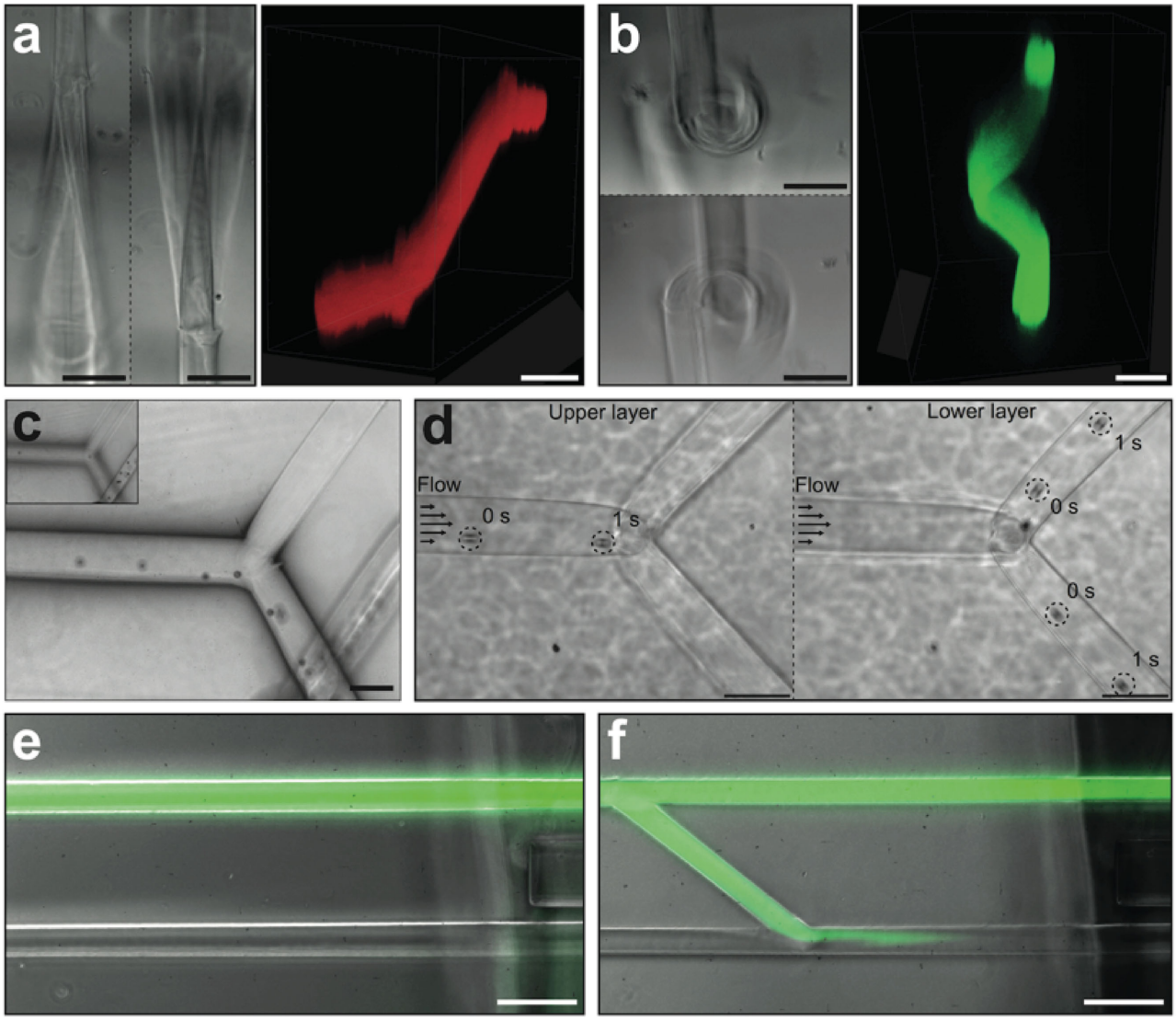

Figure 3. Three-dimensionality and evolvability of in situ biomicrofluidics. a,b) Confocal 3D reconstruction of intricate 3D microfluidic networks such as ramps or spirals. c) Representation of superimposed and aligned microfluidic networks. d) Composite image generated from Movie S3 (Supporting Information) showing polystyrene microbeads flowing through a laser-ablated microchannel. The position of microbeads in the upper and lower layer of the microfluidic network is shown at 0 and 1 s in the composite image. e) Proof-of-principle demonstration of evolving microfluidic systems. We merged a bright-field and a fluorescent image of parallel microfluidic channels. Initially, the upper channel is perfused with high-molecular-weight (2000 kDa) FITC-dextran. f) The parallel channels are then connected by laser-ablation during the perfusion. The fluorescent solution is now being directed in the lower channel. Scale bars: 100 μm.

Having demonstrated that laser-based microchannel etching is compatible with 3D cell culture, we next sought to establish 3D human MSC invasion and chemotaxis assays based on the transient, localized perfusion of the chemoattractant platelet derived growth factor-BB (PDGF-BB). Indeed, time-lapse microscopy analyses showed that directional 3D MSC migration could be selectively induced in PEG-based hydrogels upon delivery of a short pulse of PDFG-BB through a laser-ablated microfluidic channel (Figure 4d,e and Movie S4 and S5, Supporting Information). A more refined analysis of the single cell migration behavior by image analysis provided clear evidence of 3D chemotactic behavior of MSCs (Figure 4f,i).

Following, we attempted to establish a 3D MSC chemotaxis model in the context of a cell-culture format that would necessitate an in situ formation of a microfluidic network, i.e., one in which the microchannel positioning is not predetermined but rather dependent on the emergence of specific cellular behaviors (Figure S4, Supporting Information). As a proof-of-principle, we chose to grow MSCs as preformed "microtissue" aggregates composed of ≈400 cells, a format that may more faithfully mimic the physiological situation.[15] MSC microtissues were randomly encapsulated at a low density in 3D PEG hydrogels and, depending on the specific location of a microtissue of interest, we programmed the laser to ablate a microchannel in close proximity to that microtissue. Indeed, a

ADVANCED MATERIALS
www.advmat.de

www.MaterialsViews.com

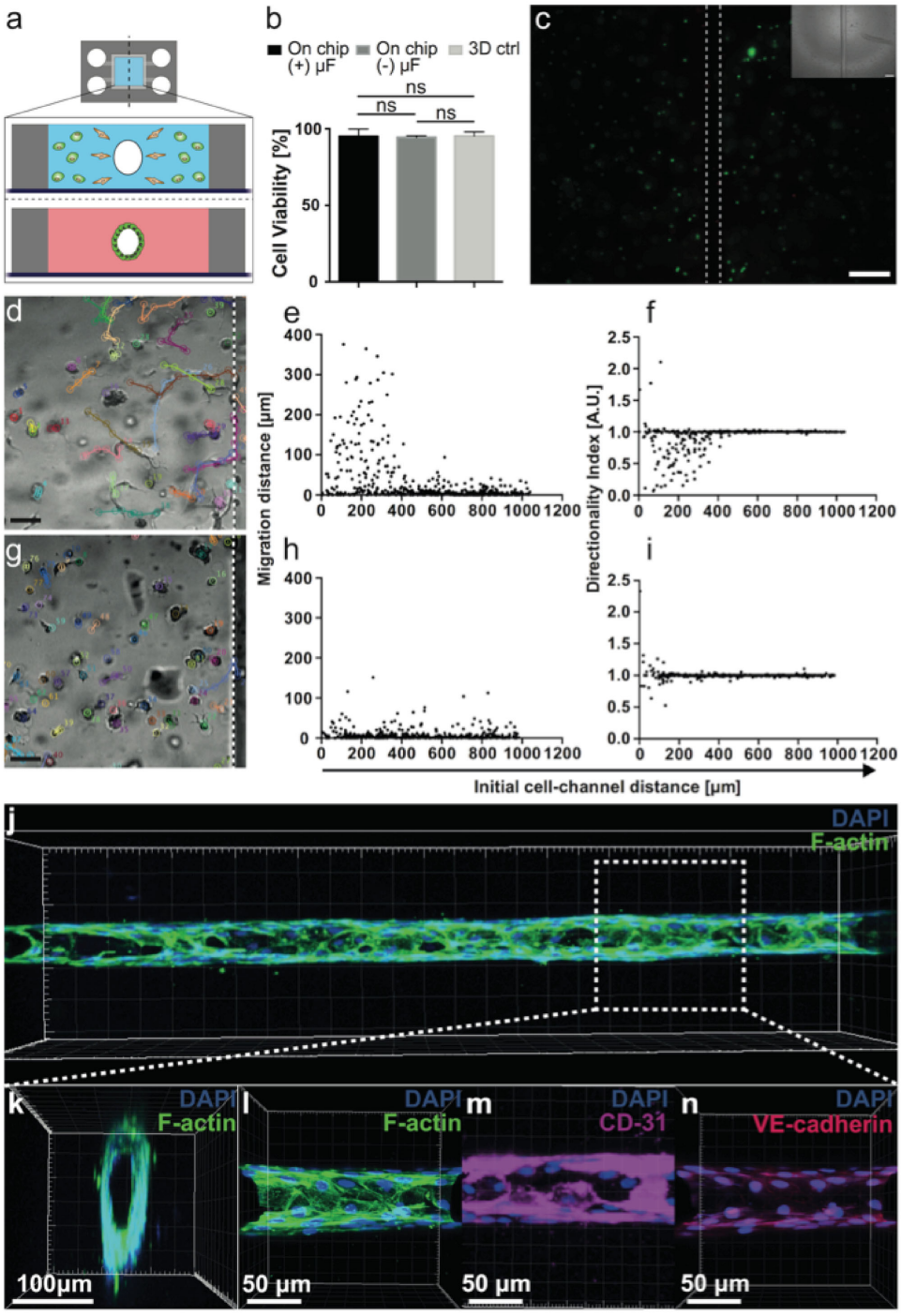

Figure 4. Applications of in situ biomicrofluidics. a) Schematic representation of the two in vitro models (3D invasion assays and blood vessel-like structures) generated here by laser-based fabrication of biomicrofluidic networks in hydrogels. b) Cell viability was assessed by live/dead staining (green fluorescence: live cells, red: dead cells) one hour after the fabrication process (N = 3, variation represented using standard deviation). Conventional 3D cultures on a 24-well plate (3D ctrl), 3D culture in the PDMS mounts without the fabricated network ((–) µF) and with the fabricated network ((+) µF) were compared. c) Wide-field fluorescent image of a representative, live/dead stained mouse myoblast (C_2C_{12}) culture. d) A representative bright-field image overlapped with the cell tracks of prestarved hMSCs perfused with PDGF-BB for 30 min. e) Analysis of the migration distance and f) the directionality index of hMSCs perfused with PDGF-BB for 30 min. g) Representative bright-field image overlapped with the cell tracks of prestarved hMSCs perfused with medium only. h) Analysis of the migration distance and i) the directionality index of hMSCs perfused with medium only. j) Confocal 3D reconstruction of a hollow endothelial cell tube (HUVECs) formed in collagen type I. k) Transversal and l) frontal plane of the structure. Frontal planes showing endothelial markers immunostainings, i.e., m) CD-31 and n) VE-cadherin.

similar 3D chemotactic behavior was observed in this experimental paradigm (Figure S4 and Movie S6 and S7, Supporting Information). Taken together, these data show that the behavior of live cells can be readily modulated by microfluidic delivery of diffusible signaling molecules. Therefore, our strategy permits the construction of functional microfluidic systems in a fully user-defined manner, based on cellular processes that are observed during a specific experiment. As such, the blueprint for the microfluidic chip is not determined a priori, but rather a posteriori, dependent on the biological question and cellular state investigated by an experimenter.

Finally, we sought to utilize laser-based photoablation to fabricate in vitro tissues. As a first model system, we decided to build user-defined, perfusable vascular networks within 3D collagen networks. A variety of such systems have already been described,[7,8] yet the state-of-the-art is based on rather complicated and time-consuming methods that possess a paucity of design flexibility and no adaptability. Here, we laser-etched microchannels into collagen type I hydrogels and seeded the channels with human-umbilical-vein endothelial cells (HUVEC) by microfluidic perfusion. Within five days, a confluent, perfusable layer of HUVEC expressing the phenotypic markers CD31 and VE-cadherin was established (Figure 4j–n). This approach could provide an elegant means to model complex phenomena in vascular or cancer biology and may also facilitate the fabrication of sophisticated 3D stem cell microenvironments containing a microvasculature.

Fabricating physiologically relevant cell culture and tissue models in vitro holds tremendous promise for applications in basic biology, drug discovery, toxicology, and regenerative medicine. However, generating in vitro models that capture even a modicum of natural tissue functionality is a formidable effort that requires sophisticated tools to control many aspects of the complex cellular microenvironment. While significant advances have been made in the development of 3D matrices that mimic key biochemical and biophysical properties of native cellular microenvironments,[16] it has not yet been possible to build in vitro systems that allow the physiological, spatiotemporally complex delivery of biomolecules in these microenvironments in an adaptable manner, that is, based on the biology that "unfolds" in the cell-culture dish. In this report, we provide the first demonstration of microfluidic networks that are fully adaptable and can be designed and fabricated in situ, according to cellular and multicellular events observed during an experiment.

Compared to existing strategies based on micromoulding and sacrificial layer elimination (e.g., refs. [6,8]), our approach shows several distinct advantages. First, no complex steps are involved in the fabrication of microfluidic networks. Hydrogels of choice can be formed in a perfusion chamber, fluid networks fabricated by laser etching and perfusion directly performed by connecting to a tubing system integrated in a world-to-chip interface. As the process can be performed without the need of an operator, this method significantly decreases the tedious aspect of microfluidic chip fabrication, requiring only equipment that is readily available at most research institutes. Second, since light is used for the fabrication, the sterility of the cell cultures is guaranteed. Finally, the fabrication of microfluidic networks is not restricted in geometry and complexity. We think that the presented strategy represents an important step forward in the implementation of miniaturized, near-physiological cell and tissue culture platforms to answer currently unresolved questions in biomedical research as well as the ability to guide cellular self-organization to form functional tissues in vitro.

Experimental Section

Preparation of Hydrogels: PEG hydrogels crosslinked via Michael-type addition reaction (termed "MT-gel" in the Supporting Information) were prepared as described,[17] mixing aqueous solutions containing thiol- and vinylsulfone-functionalized four- and eight-arm PEG macromers (mol. weight 10 and 40 kDa, respectively) at various concentrations to adjust stiffness and stoichiometric ratio.

PEG hydrogels crosslinked via thrombin-activated transglutaminase factor XIIIa (FXIIIa) (termed "TG-gel" in the Supporting Information) were prepared as previously described.[18,19] Briefly, eight-arm PEG macromers (40 kDa) bearing lysine- or glutamine-containing FXIIIa substrate peptides were mixed at various concentrations to adjust the stiffness and the stoichiometric ratio. For 3D cell-culture experiments, FXIIIa-based PEG hydrogels were synthesized bearing matrix-metalloprotease-sensitive as well as integrin-binding peptides.[19] Hydrogel precursor solutions were pipetted into the hydrogel chamber of the PDMS mounts. After crosslinking, buffer or appropriate medium was added to allow equilibration of the hydrogel.

Native bovine dermis collagen type I (5 mg mL^{-1} stock concentration, Kouken, Japan) was reconstituted according to the manufacturer's protocol. The water content was adjusted to obtain the appropriate concentration and variable mechanical properties.

Fabrication of Microfluidic Networks via Laser Ablation: A nanosecond laser system was used for the fabrication of microfluidic networks in hydrogels: a PALM MicroBeam system (1 ns pulses, 100 Hz frequency, 355 nm) from Carl Zeiss Microscopy (Göttingen, Germany) set with a 10× objective (NA = 0.25) and a constant stage speed, 95 μm s^{-1}, was used in all experiments. To fabricate planar microfluidic networks, the built-in interface, including software connected to the laser, as well as an automated stage to control the laser position, was used. The patterns were drawn as vectorial designs of the shape of interest, which can be created in any vectorial drawing software (here Adobe Illustrator CS6). The designs were then converted to the microscope specific format using a custom-made converter before being imported onto the PALM MicroBeam system's interface. The laser was then started and the network was fabricated similarly to previously described work by Sarig-Nadir et al.[11]

To fabricate 3D microfluidic networks, the same strategy was adopted. In addition, a custom-made *z*-controller was fabricated using a bipolar stepper motor interfaced with Arduino microcontrollers (Arduino Uno & Arduino Motor Shield). The laser's host system and *x*-*y* stage were coordinated with the stepper motor to achieve a coherent 3D network fabrication. Finally, the size of the microfluidic network could be varied by increasing the volume scanned by the laser. The 2D and 3D microfluidic networks were imaged by wide-field microscopy as well as confocal microscopy.

Supporting Information

Supporting Information is available from the Wiley Online Library or from the author.

Acknowledgements

The authors thank Tunvez Boulic and Marie-Laure Naudin for help with the characterization of biomolecule diffusion through hydrogels and the

characterization of the artificial vasculature network, respectively. The authors thank Michael Snyder, Nikolce Gjorevski, and Andrea Manfrin for helpful discussions and critical reading of the manuscript, and Sylke Höhnel for contributions to the figure design. This work was funded by the EU framework 7 HEALTH research programme PluriMes (http://www.plurimes.eu/), the SystemsX.ch RTD project StoNets, an ERC grant (StG_311422), and a Swiss National Science Foundation Singergia grant (CRSII3_147684).

Received: February 25, 2016
Published online: June 23, 2016

[1] C. Frantz, K. M. Stewart, V. M. Weaver, *J. Cell Sci.* **2010**, *123*, 4195.
[2] a) F. Crick, *Nature* **1970**, *225*, 420; b) J. B. Gurdon, P. Y. Bourillot, *Nature* **2001**, *413*, 797.
[3] a) S. N. Bhatia, D. E. Ingber, *Nat. Biotechnol.* **2014**, *32*, 760; b) E. K. Sackmann, A. L. Fulton, D. J. Beebe, *Nature* **2014**, *507*, 181; c) T. Dvir, B. P. Timko, D. S. Kohane, R. Langer, *Nat. Nanotechnol.* **2011**, *6*, 13.
[4] a) K. J. Regehr, M. Domenech, J. T. Koepsel, K. C. Carver, S. J. Ellison-Zelski, W. L. Murphy, L. A. Schuler, E. T. Alarid, D. J. Beebe, *Lab Chip* **2009**, *9*, 2132; b) E. Berthier, E. W. Young, D. Beebe, *Lab Chip* **2012**, *12*, 1224.
[5] a) D. H. Nguyen, S. C. Stapleton, M. T. Yang, S. S. Cha, C. K. Choi, P. A. Galie, C. S. Chen, *Proc. Natl. Acad. Sci. USA* **2013**, *110*, 6712; b) A. P. Golden, J. Tien, *Lab Chip* **2007**, *7*, 720; c) J. Isern, B. Martin-Antonio, R. Ghazanfari, A. M. Martin, J. A. Lopez, R. del Toro, A. Sanchez-Aguilera, L. Arranz, D. Martin-Perez, M. Suarez-Lledo, P. Marin, M. Van Pel, W. E. Fibbe, J. Vazquez, S. Scheding, A. Urbano-Ispizua, S. Mendez-Ferrer, *Cell Rep.* **2013**, *3*, 1714.
[6] N. W. Choi, M. Cabodi, B. Held, J. P. Gleghorn, L. J. Bonassar, A. D. Stroock, *Nat. Mater.* **2007**, *6*, 908.
[7] J. P. Morgan, P. F. Delnero, Y. Zheng, S. S. Verbridge, J. Chen, M. Craven, N. W. Choi, A. Diaz-Santana, P. Kermani, B. Hempstead, J. A. Lopez, T. N. Corso, C. Fischbach, A. D. Stroock, *Nat. Protoc.* **2013**, *8*, 1820.
[8] J. S. Miller, K. R. Stevens, M. T. Yang, B. M. Baker, D. H. Nguyen, D. M. Cohen, E. Toro, A. A. Chen, P. A. Galie, X. Yu, R. Chaturvedi, S. N. Bhatia, C. S. Chen, *Nat. Mater.* **2012**, *11*, 768.
[9] a) A. Kloxin, A. M. Kasko, C. N. Salinas, K. Anseth, *Science* **2009**, *324*, 59; b) R. G. Wylie, S. Ahsan, Y. Aizawa, K. L. Maxwell, C. M. Morshead, M. S. Shoichet, *Nat. Mater.* **2011**, *10*, 799; c) K. A. Mosiewicz, L. Kolb, A. J. van der Vlies, M. M. Martino, P. S. Lienemann, J. A. Hubbell, M. Ehrbar, M. P. Lutolf, *Nat. Mater.* **2013**, *12*, 1072; d) C. A. DeForest, D. A. Tirrell, *Nat. Mater.* **2015**, *14*, 523.
[10] a) S. D. Gittard, R. J. Narayan, *Expert Rev. Med. Devices* **2010**, *7*, 343; b) C. Liu, Y. Liao, F. He, Y. Shen, D. Chen, Y. Cheng, Z. Xu, K. Sugioka, K. Midorikawa, *Opt. Express* **2012**, *20*, 4291.
[11] O. Sarig-Nadir, N. Livnat, R. Zajdman, S. Shoham, D. Seliktar, *Biophys. J.* **2009**, *96*, 4743.
[12] a) O. Ilina, G.-J. Bakker, A. Vasaturo, R. M. Hoffman, P. Friedl, *Phys. Biol.* **2011**, *8*, 029501; b) M. B. Applegate, J. Coburn, B. P. Partlow, J. E. Moreau, J. P. Mondia, B. Marelli, D. L. Kaplan, F. G. Omenetto, *Proc. Natl. Acad. Sci. USA* **2015**, *112*, 39.
[13] F. Ramirez, D. B. Rifkin, *Matrix Biol.* **2003**, *22*, 101.
[14] P. Bianco, X. Cao, P. S. Frenette, J. J. Mao, P. G. Robey, P. J. Simmons, C. Y. Wang, *Nat. Med.* **2013**, *19*, 35.
[15] F. A. Saleh, P. G. Genever, *Cytotherapy* **2011**, *13*, 903.
[16] a) C. A. DeForest, K. S. Anseth, *Annu. Rev. Chem. Biomol. Eng.* **2012**, *3*, 421; b) N. Gjorevski, A. Ranga, M. P. Lutolf, *Development* **2014**, *141*, 1794.
[17] S. Gobaa, S. Hoehnel, M. Roccio, A. Negro, S. Kobel, M. P. Lutolf, *Nat. Methods* **2011**, *8*, 949.
[18] a) M. Ehrbar, S. C. Rizzi, R. Hlushchuk, V. Djonov, A. H. Zisch, J. A. Hubbell, F. E. Weber, M. P. Lutolf, *Biomaterials* **2007**, *28*, 3856; b) M. Ehrbar, S. C. Rizzi, R. G. Schoenmakers, B. S. Miguel, J. A. Hubbell, F. E. Weber, M. P. Lutolf, *Biomacromolecules* **2007**, *8*, 3000.
[19] M. Ehrbar, A. Sala, P. Lienemann, A. Ranga, K. Mosiewicz, A. Bittermann, S. C. Rizzi, F. E. Weber, M. P. Lutolf, *Biophys. J.* **2011**, *100*, 284.